A Study Of Three Fault Dynamics Parameters Associated With The Seismicity Of Mid-Ocean Ridge System

Olatunde Isaiah Popoola and Nicholas Irabor Adimah

Department Of Physics, University of Ibadan, Ibadan, Nigeria
nickydof@yahoo.com

Abstract: Mid-ocean ridges are sources of moderate and shallow earthquakes. The possible relationships between radiated energy per area (ξ) of earthquakes occurring along these ridges and certain defined fault dynamics parameters namely ridge spreading speed (Υ), kinetic energy factor (Ω) and angle of deviation from normal ridge divergence (Θ) were investigated for the mid-Atlantic and Indian Ocean ridge using a fifty year earthquake data. The study area was divided into 27 regions and a radiated earthquake energy model was used to obtain ξ for each region while Ω was calculated from Υ and a parameter that is a measure of the lithospheric mass of the region in kilogram. The results revealed a general increase in seismicity in 25 out of the 27 regions. Correlations of ξ with Υ, Ω and Θ showed high degree of randomness, indicating that additional factors believed to be unique to each region may influence the seismicity process.
[Olatunde Isaiah Popoola and Nicholas Irabor Adimah. **A Study Of Three Fault Dynamics Parameters Associated With The Seismicity Of Mid-Ocean Ridge System.** *Nat Sci* 2015;13(8):105-110]. (ISSN: 1545-0740). http://www.sciencepub.net/nature. 17

1.   Introduction

The diversity of seismicity patterns together with the difficulty of establishing if certain variations of seismic activity are genuine, statistically significant and correlate with some physical observables are important reasons why the processes that control the occurrence of earthquakes are poorly understood and under continuous debate (Enescu *et al*., 2009). Plate tectonic explains a large portion of the world's seismicity, since more than 90% of the seismicity occurs on plate margins. The kinematics of the lithosphere are the primary constraints on its dynamics and on the kinematics and the dynamics of the deeper solid earth. As a result, determination of plate motions has been a major research area since the formation of plate tectonics (Stein, 1993). In the past years, space-based geodetic observations have acquired comparable significance in plate tectonic studies. The result of the crustal dynamic project, show the range of techniques that have been used and results that have been derived (Stein, 1993).

Understanding the physics of earthquakes requires relating the dynamics of faulting with seismological and physically observable parameters. One of these observables (which is one of the most fundamental parameters for describing an earthquake) is the radiated seismic energy E. It is an indication of the total wave energy generated by the rapid rupture of an earthquake (Venkataraman and Kanamori, 2004). Thus, E is a valuable parameter, useful for understanding the dynamic rupture, particularly in the case of large and complex slow source earthquakes. The radiated energy, and hence energy magnitude, Me (Choy and Boatwright, 1995), is also useful for rapid real‑time

hazard assessment and damage mitigation as it does not saturate, and only requires the arrival of the initial P wave group for determinations in as little as 5 to 10 minutes at near‑teleseismic distances (25° to 50°) (Newman *et al*., 2011). In practice, energy has historically almost always been estimated with empirical formulas. Prior to the worldwide deployment of broadband seismometers, which started in the 1970s, most seismograms were recorded by conventional seismographs with narrowly peaked instrument responses. The difficulties in processing analogue data were thus compounded by the limitations in retrieving reliable spectral information over a broad bandwidth. Fortunately, theoretical and technological impediments to the direct computation of radiated energy have been removed.

Several studies have been carried out in the past to ascertain seismicity patterns and how they correlate with some physical parameters in different parts of the world. In the work of Papazachos, (1999), Greece and the surrounding area were organized into a grid, the 'a' and 'b'-values were simultaneously determined for the whole grid by solving an appropriate linear system. The results obtained were in good agreement with previous studies and further enhanced the knowledge of the study area. In another study, Drakopoulous (1968) divided the region of Greece into many parts and obtained 'b'-value for each division. His results showed that for almost all parts, 'b'-values ranged between 0.4 and 1.7. He inferred from this study that 'b'-value varies much more vertically than horizontally. Some researchers are of the view that 'b'-value varies from 0.5 to 1.0 for tectonic earthquakes and a higher 'b'-value for volcanic events (Gresta and

Patane, 1983). Studies by Hurtig and Stiller (1984), Udias and Mezcua (1997) on global seismicity revealed that 'b'-value ranges from 0.3 to 1.8 and 0.8 to 1.2 respectively. The study of the mining tremors and tectonic earthquakes in South Africa (McGarr, 1984) showed that 'b'-values ranged from 0.6 to 1.5. The higher the 'a'-value in a given region, the higher the seismicity.(Nuannin, 2006)

Enescu *et al*., (2009) investigated the relationship between properties of seismicity pattern in southern California and the surface heat flow using a relocated earthquake data. It was discovered that the spatial distribution of α (the productivity parameter) generally correlate well with surface heat flow. Adedeji (2012) developed two models for rating seismic activities using radiated earthquake energy. Using the developed models and the G-R relation, seismic activities of ten areas in the world seismic zones were rated. Hammed (2005) investigated global seismicity across the equator and observed that going from north to south, global seismicity increased suddenly after crossing the equator.

Table 1. Discretization of the study area

REGION	MAX.LAT.	MIN.LAT.	MAX.LONG.	MIN.LONG.
1	82.5	75.0	10.0	-5.0
2	75.0	70.0	10.0	-15.0
3	70.0	62.5	-13.0	-25.0
4	65.0	52.0	-25.0	-37.0
5	50.0	43.0	-25.0	-30.0
6	42.5	35.0	-22.5	-37.5
7	35.0	15.0	-35.0	-50.0
8	15	2.5	-30	-47.5
9	2.5	-2.5	-10.0	-32.5
10	-2.5	-32.5	-10.0	-17.5
11	-32.5	-45	-15.0	-20.0
12	-45.0	-52.5	-7.5	-15.0
13	-52.5	-62.5	-5.0	-35.0
14	-50.0	-57.5	22.5	-5.0
15	-40.0	-55.0	40.0	22.5
16	-27.5	-45.0	63.0	40.0
17	2.5	-27.5	72.5	63.0
18	10.0	2.5	67.5	57.5
19	17.5	10.0	60.0	40.0
20	-55.0	-65.0	-35.0	-70.0
21	-47.5	-57.5	-112.5	-122.5
22	-52.5	-57.5	-122.5	-140.0
23	-55.0	-62.5	-140.0	-152.5
24	-62.5	-67.5	-155.0	-175.0
25	-60.0	-67.5	-175.0	160.0
26	-50.0	-65.0	157.5	137.5
27	-42.5	-55.0	132.5	90.0

Rundquist and Sobolev, (2002) summarized the principal result of the studies in mid-ocean ridge (MOR) seismicity and their implications for geodynamics. It was obtained that the relationship between the seismic moment released, fault length and spreading rate were quite different for transform and rift parts of MOR; this confirms the difference in the geometry of their respective earthquake source volumes with the principal factor controlling the ridge seismicity being the thermal structure of the lithosphere. Time-clustering behaviour of spreading centre seismicity between 15^0 and 35^0N on the mid-Atlantic ridge: observations from hydro-acoustic monitoring (Bohnenstiehl *et al*., 2003) indicated that the distribution of inter-event times is consistent with a non-periodic, non-random, clustered process with the highest degrees of clustering associated temporally with large mainshock-aftershock sequence.

2.   Material and Methods

Several data sets ranging from earthquake data to plate motion data were used in carrying out this research.

a)   Earthquake data

The earthquake data used were obtained from the earthquake catalogue of the Advanced National Seismic System (ANSS), a website of Northern California Earthquake Data Centre, USA. The obtained data contained over 25,000 natural earthquakes occurring along the mid-ocean ridges with magnitude $2.0 \leq M \leq 9.0$ from January 1st, 1963 to December 31st, 2012 (period of 50 years). The data for individual earthquakes contained date of occurrence, time of occurrence, latitude and longitude of the epicentre, the depth, the magnitude and the magnitude type.

b)   Ridge spreading speed (ϒ) data

The Lamont-Doherty plate velocity calculator was used to generate the following data for each of the 27 regions: the north and east spreading velocities, the resultant spreading speed of the ridge in mm/yr, the relative plate motion model, the azimuth of the chosen point on the ridge and the plates bounding the chosen point on the ridge.

c)   Spatial distribution of lithospheric thickness

The spatial distribution of lithospheric thickness was obtained from the Conrad and Lithgow-Bertelloni (2006) model for lithospheric thickness. The data for each point contained: The longitude, the latitude and the lithospheric thickness of the selected point.

The whole of the study area (mid-Atlantic ridge, pacific-Antarctic ridge, southeast Indian ridge, southwest Indian ridge and mid-Indian ridge) was discretized into 27 regions. The longitudinal and latitudinal boundaries of the regions are shown in Table

1 and their locations on the global seismicity map are shown in Figure 1.
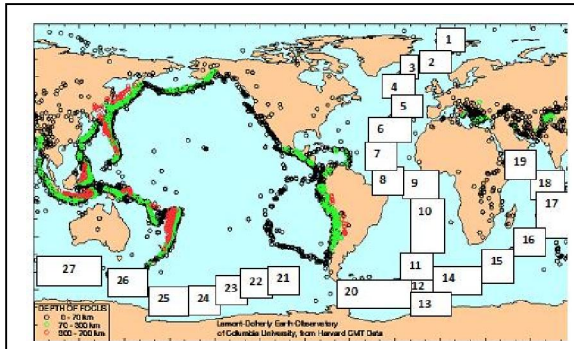
Figure 1. Global Seismicity Map (Harvard CMT DATA, 2000) with the Regions of Study Inscribed

The earthquake data were recorded in different magnitude types in the catalogue. These were all converted to the moment magnitude (M_w) using the following empirical relations:

$0.80M_L - 0.60M_s = 1.04$ or $M_s = 1.33M_L - 1.73$ 1

(Ambraseys and Boomer, 1990)

$M_b = M_s + 1.33$, $M_s < 2.86$ 2

$M_b = 0.67 M_s + 2.28$, $2.86 < M_s < 4.90$ 3

$M_b = 0.33 M_s + 3.91$, $4.90 < M_s < 6.27$ 4

$M_b = 6.00$, $6.27 > M_s$ 5

$Log M_o = M_s + 18.89$, $M_s < 6.76$ 6

$Log M_o = 1.5 M_s + 15.51$, $6.76 < M_s < 8.12$ 7

$Log M_o = 3 M_s + 3.33$, $8.12 < M_s < 8.22$ 8

$M_s = 8.22$, $Log M_o > 28$ 9
(Geller, 1976)

$Log M_o = 1.5 M_w + 16.1$ 10
(Kanamori, 1977)

$M_e = 0.3 + Ms$ 11
(USGS, 2000)

The total radiated energy of earthquakes per unit area, A, for each region was calculated using:

$$\xi = \sum_i^N \frac{10^{(1.5m_i + 11.8)}}{A}$$ 12

Where m = Mw, N is the number of earthquakes (Adedeji, 2012). Equation 12 results from the equation of the radiated energy (E) of earthquakes (Kanamori, 1977);

$Log E = 1.5Mw + 11.8$ 13

The kinetic energy factor (Ω) is a fault dynamics parameter defined to be proportional to the average kinetic energy of the ridge and was obtained for each of the regions using:

$$\Omega = \frac{1}{2}M\gamma^2$$ 14

Where M is the lithospheric mass of the ridge in kilogram obtained from average lithospheric density and volume for each region and Υ is the average ridge spreading speed.
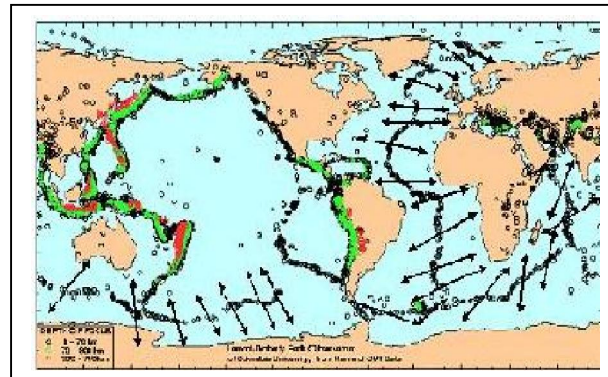
Figure 2. Global seismicity map showing directions of ridge spreading (Harvard CMT DATA, 2000)
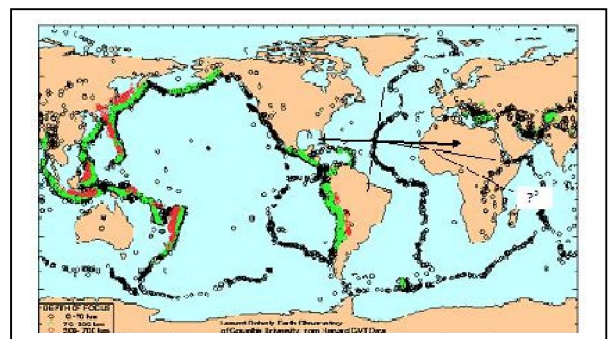
Figure 3. Global Seismicity map showing a typical angle of deviation from normal divergence (Θ^0) (not drawn to scale).

The angle of deviation from normal divergence, Θ^0, was obtained geometrically for each of the regions as shown in Figure 3. Graphs showing the temporal variation of radiated energy per area for each of the regions in steps of 10 years were plotted and the methods of freehand and least square were employed in the general trend estimation. Each of the three fault dynamics parameters defined in this work, viz; ridge

spreading speed (ϒ), kinetic energy factor (Ω) and the angle of deviation from normal divergence (Θ⁰) was also plotted against the radiated earthquake energy per area to see if there is any correlation.

3.   Results

The graphs showing the temporal variation of radiated energy for the whole of the mid-oceanic ridges are shown in Figure 4(i-vi). R1-27 stands for regions 1-27. The relationships between the three fault dynamics parameters and the radiated energy of earthquakes per area are shown in Figures 5 – 7.
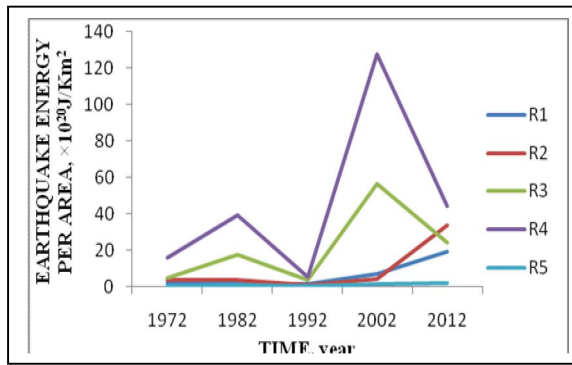
(i)
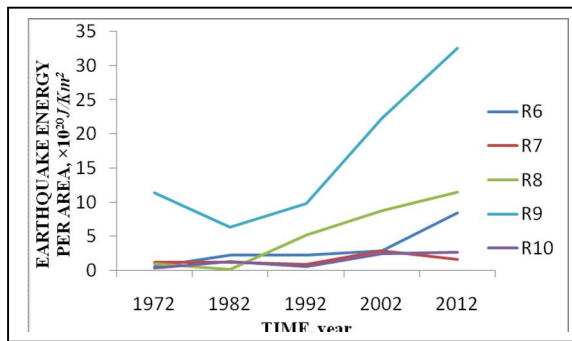
(ii)
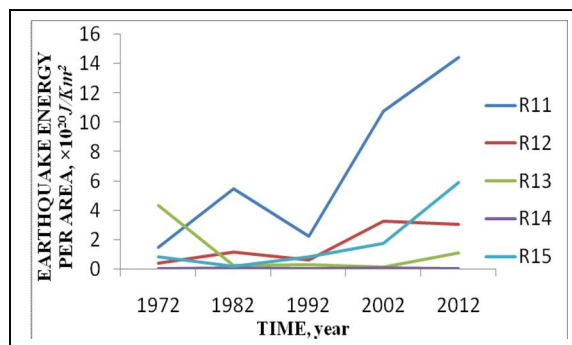
(iii)
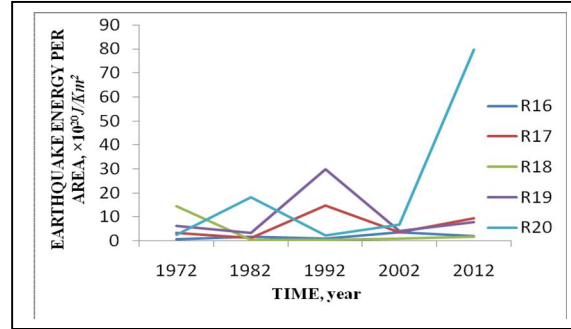
(iv)

Figure 4 (i-vi). Temporal variation of radiated earthquake energy
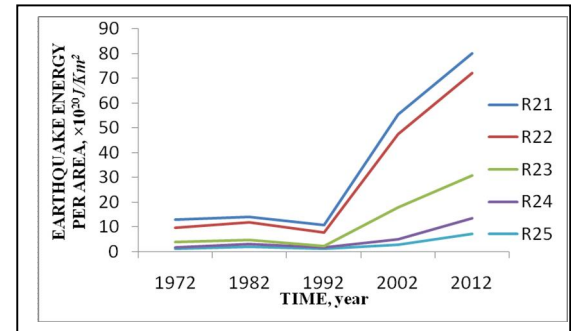
(v)
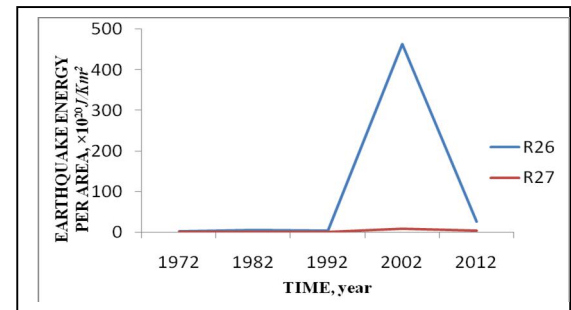
(vi)
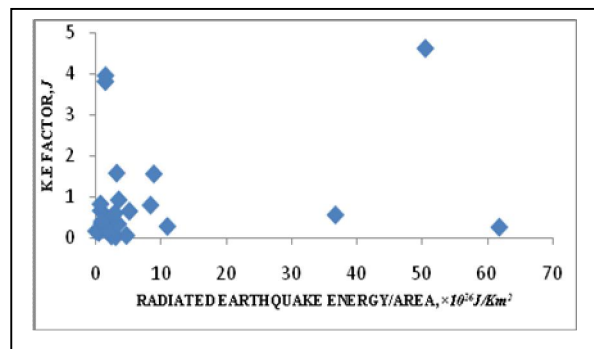
Figure 5. A graph of kinetic energy factor against radiated earthquake energy per area

108
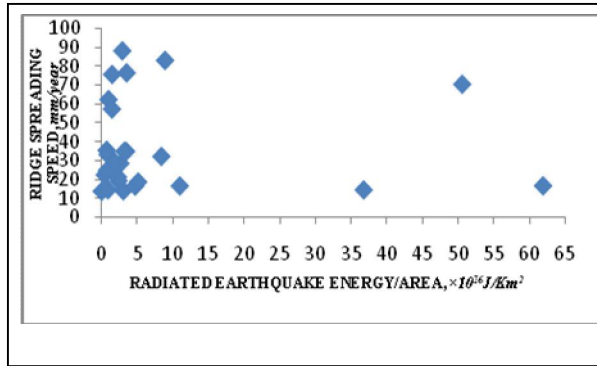
Figure 6. A graph of ridge spreading speed against radiated earthquake energy/area
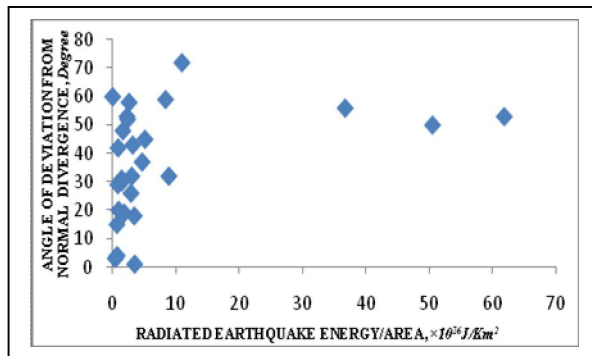
Figure 7. A graph of angle of deviation from normal divergence against radiated earthquake energy/area

4.   Discussions

The temporal variation of radiated earthquake energy per area for each of the 27 regions is unique; no two regions exhibited a similar pattern. However there was a general increase in this quantity over the whole time window which is an indication of increasing seismicity in the mid-oceanic ridge system and 1992 constituted a year of low earthquake radiated energy for all the regions except regions 17 and 19. The relationship between the radiated earthquake energy per area (ξ) with each of the defined fault dynamics parameters; ridge spreading speed or rate (Υ), kinetic energy factor(Ω) and angle of deviation from normal divergence (Θ^0) appears to be random as can be seen in Figures 5, 6 and 7.

There is no reliable pattern of relationship between the radiated earthquake energy and the three dynamics parameters defined in this work. This implies that within the 50-year period examined, the investigated parameters were not dominant features which shaped seismicity in the region. Other factors such as magma budget (which is known to correlate well with the highly variable ridge spreading speed in most regions), rock type etc may have more influence on the seismicity of the region. Meanwhile, the 1992 low earthquake radiated energy observed for most of the mid-oceanic ridge system seems to be a striking feature which may be an indication of self organisation in the complex process of energy build-up in the ridges.

Corresponding Author:
Nicholas Irabor Adimah
Department of Physics
University of Ibadan
Nigeria
Email: nickydof@yahoo.com
Tel.: +234(0)8064275352
Author: O.I. Popoola
Email address: itundepopoola@yahoo.com
Tel.: +234(0)8023217050

References
1. Adedeji A. O. (2012): "Development of models for rating seismic activities using radiated energy of earthquakes". Ph.D thesis submitted to the Department of Physics, University of Ibadan.
2. Bilham R., (1991). Earthquakes and sea level: crustal deformation metrology on a changing planet, *Rev. Geophys*., 1, 1-29, Feb 1991.
3. Bohnenstiehl D.R., Tolstoy M., Smith D.K., Fox C.G. and Dziak R.P. (2003): Time clustering behavior of spreading-center seismicity between 15^0 and 35^0N on the mid-Atlantic ridge: observations from hydro-acoustic monitoring. Physics of the earth and planetary interiors: 138 (2003) 147-161.
4. Chase C. G. (1978). Plate kinematics: The Americas, East Africa and the rest of the world, Earth planet. Sci. lett., 37, 355-368.
5. Choy G. L. and Boatwright, J. L. (1995): Global patterns of radiated seismic energy and apparent stress. J. Geophys. Res., 100, 89, 205-18,228.
6. Drakopoulus J. C. (1968). Characteristics parameters of fore- and aftershock sequences in the region in Greece. 1-29 in Drakapoulus J.C. and Ekonomides A.C.
7. Enescu B., Hainzl S. and Ben-Zion Y. (2009): "Correlations of seismicity patterns in southern California with surface Heat Flow Data". Bull. Seismol. Soc. Am., Vol. 99, No. 6, pp. 3114-312.
8. Gresta S. and Patane G. (1983). Variation of b-values before the Etnean Eruption of march 1981. Pageophy, 121:2, 288-295.
9. Hammed A. K. (2005): "Investigation of global seismicity across the equator". M.Sc. thesis submitted to the Department of Physics, University of Ibadan.
10. Hurtig E. and Stiller H. (1984): "Erdbeben und Erdbebengerfahrdung". AkademiieVerlag Berlin, pp. 328.

11. Kanamori H. (1977): "The energy released in great earthquakes". Journal of Geophysics Research, 82: 2981-2876.
12. Lowrie W. (1997).Fundamentals of geophysics. Cambridge: Cambridge University press.
13. McGarr A. (1984): "Some application of seismic source mechanism studies to assessing underground harzard. In: N.C. Gay and E.H Wainwright (Eds.)". Proc. 1st inter. Congress on rockbursts and seismicity in mines.SAIM Johannesburg, pp.199-208.
14. Newman A.V., G. Hayes, Y. Wei and J.A. Convers (2011). The 25 October 2010 Mentawai tsunami earthquakes. J. Geophys. Res., 103, 26, 885-26,898.
15. Nuannin P. (2006). The potential of b-value variations as earthquake precursors for small and large events.Digital comprehensive summaries of
16. Uppsala Dissertation, from the faculty of science and technology.
17. Oncel A. O. and Wilson T. H. (2002). Space-time correlations of seismotectonic parameters: examples from japan and from turkey preceding the Izmit earth quake time correlations of seismotectonic parameters: Bul. of the seismol. Soc Of Am, vol. 92, no. 1339-1349.Doi: 1785/1020000844.
18. Papazachos C. (1999): "An alternative method for reliable estimation of seismicity with an application in Greece and the surrounding area". Bulletin of the seismological society of America, vol. 89; no. 1, pp.111-119.
19. Rundquist D.V. and Sobolev P.O. (2002): Seismicity of mid-ocean ridges and its geodynamics implications: a review. Earth-science reviews 58, 143-161.
20. Stein S. (1993). Space geodesy and plate motions, in Contributions of Space Geodesy to Geodynamics: Crustal Dynamics, Geodyn. Ser., vol. 23, edited by D.E. Smith and D. L. Turcotte, pp. 5–20, AGU, Washington, D. C., doi:10.1029/GD023p0005.
21. Udias A. and Mezcua J. (1997): "Fundamentos de Geofisca. Alianza Universidad Textos, . 476
22. Venkataraman A. and Kanamori H. (2004): Observational constraints on the fracture energy of subduction zone earthquakes. J. Geophys. Res., 109, B05302, doi: 10.1029/2003JB002549.
23. Wiemer S., McNutt S.R. and Wyss M. (1998): "Temporal and 3-D spatial analysis of the frequency-magnitude distribution near Long Valley Calder, California". Geophysics journal international, 134: 409-421.

8/1/2015